Available online at www.sciencedirect.com
SCIENCE DIRECT®
Journal of Invertebrate Pathology 90 (2005) 122–126
Journal of INVERTEBRATE PATHOLOGY
www.elsevier.com/locate/yjipa

Short communication

Ultrastructural analysis supports transferring *Nosema whitei* Weiser 1953 to the genus *Paranosema* and creation a new combination, *Paranosema whitei*

Yuliya Y. Sokolova [a,*], Irma V. Issi [b], Elena V. Morzhina [c], Yuriy S. Tokarev [b], Charles R. Vossbrinck [d]

[a] *Institute of Cytology, 194064 St. Petersburg, Russia*
[b] *Institute for Plant Protection, 196608 St. Petersburg, Russia*
[c] *Institute of Physiology and Biochemistry , 1944064 St. Petersburg, Russia*
[d] *Connecticut Agricultural Experiment Station, New Haven, CT 06511, USA*

Received 27 April 2005; accepted 8 June 2005
Available online 3 August 2005

Abstract

The current ultrastructural description of *Nosema whitei* is in agreement with the genus definition of *Paranosema* [Sokolova, Y.Y., Dolgikh, V.V., Morzhina, E.V., Nassonova, E.S., Issi, I.V., Terry, R.S., Ironside, J.E., Smith, J.E., Vossbrinck, C.R., 2003. Establishment of the new genus *Paranosema* based on the ultrastructure and molecular phylogeny of the type species *Paranosema grylli* Gen. Nov., Comb. Nov (Sokolova, Selezniov, Dolgikh, Issi 1994), from the cricket *Gryllus bimaculatus* Deg. Journal of Invertebrate Pathology 84, 159–172]. In addition to exhibiting similar spore morphology and sporogony type, *N. whitei*, like *P. grylli* and *Paranosema locustae,* possesses a distinct meront–sporont transitional stage in the life cycle; develops in the host fat body, and produces secretory material arranged in "tubular structures" during sporogony. Ultrastructural analysis supports the similarity of *N. whitei* to *P. grylli* and to *P. locustae* as predicted on the basis SSrDNA sequence data (GenBank Accession Nos. AY305323, AY305325, and AY305324). Comparative studies of these three related species provide a good example of the consistency of morphological and sequence data, and support both the placement of *N. whitei* inside the genus *Paranosema* and the validity of the new combination *Paranosema whitei* (Weiser) . Supported by Russian Foundation for Basic research: Grants 04-04-49314 and 03-04-49629.

Keywords: *Nosema whitei*; *Paranosema grylli*; *Paranosema locustae*; *Tribolium* sp.; Microsporidia; Ultrastructure; Phylogeny

1. Introduction

Comparative phylogenetic analysis of SSrDNA showed that *Nosema grylli* (GenBank Accession No. AY305324), a microsporidian parasite of the cricket *Gryllus bimaculatus*, is closely related to *Nosema locustae* (GenBank Accession No. AY305325), and to *Nosema whitei* (GenBank Accession No. AY305323) from flour beetles, *Tribolium* spp. (Sokolova et al., 2003). The sequence divergence and morphological traits clearly separate this group of parasites from the "true" *Nosema* clade with *Nosema bombycis* as a type species, which parasitizes mainly lepidopterans. The generic name of *N. grylli* and its close relative *N. locustae* therefore has been changed to *Paranosema*. *N. whitei* Weiser 1953 was left in its original status due to lack of data on fine morphology (Sokolova et al., 2003). Very few details of the *N. whitei* ultrastructure were resolved in the pioneer work

* Corresponding author. Present address: Department of Ento mology, Louisiana State University, Baton Rouge, LA 70803, USA. Fax: +1 225 578 1643, +011 7 812 247 03 41..
E-mail addresses: jsokolova@lsu.edu, jumicro@yahoo.com (Y.Y. Sokolova).

0022-2011/$ - see front matter © 2005 Published by Elsevier Inc.
doi:10.1016/j.jip.2005.06.009

of Milner (1972a), one of the earliest applications of transmission electron microscopy to microsporidia. The goal of this paper is to present updated ultrastructural data on *N. whitei*, and to establish its proper classification, in this case, a new combination, *Paranosema whitei* (Weiser).

2. Materials and methods

Microsporidial infection naturally occurred in a population of flour beetles, *Tribolium castaneum*, infesting private flour storage in St. Petersburg. Observation of fresh smears and Giemsa-stained preparations made from the infected insects allowed identification of the microsporidium as *Nosema whitei* based on slide collection of Irma V. Issi (All Russian Institute for Plant Protection, St. Petersburg, Russia). Dry microsporidia-killed *T. castaneum* specimens, heavily loaded with spores, were collected and refrigerated until use. Healthy cultures of *T. castaneum* were obtained from the insectarium of the Institute of Plant Protection, St. Petersburg, Russia. Insects were reared at 25 °C on a diet containing four parts of oatmeal and one part of dried yeast, with vegetable or fruit peelings to supply moisture. For experimental infection, dried infected specimens were ground to a powder in a mortar. The powder was washed several times by centrifugation, the resultant pellet consisting mostly of mature *N. whitei* spores. The final suspension containing approximately 10^6 spore/ml was mixed with the rearing medium and the beetles were exposed to this mixture. In 40 days, larvae and adults were checked for the presence of microsporidia spores. The infected individuals were dissected under the dissecting microscope, and their fat bodies were removed and processed for routine electron microscopy (Sokolova et al., 2003). Fresh or methanol fixed and stained with Trichrom or Giemsa, smears of microsporidia-infected insects were photographed and measured under Nikon Eclipse E-600 Microscope equipped with a Metaview digital camera and software (MetaView. 1998, Meta Imaging Series 4.5. Universal Imaging Corporation, West Chester, PA).

3. Results and discussion

3.1. Spore measurements

Living spores measured from 3.87 to 4.97 μm in length, and from 2.46 to 3.12 μm in width, averaging $4.64 \pm 0.098 \times 2.85 \pm 0.074$ μm ($x \pm$ SE, $n = 11$), with a width/length ratio of 0.62 ± 0.015 μm. Methanol fixed spores measured from 3.78 to 4.62 μm in length, and from 2.37 to 3.05 μm in width, averaging $4.19 \pm 0.067 \times 2.62 \pm 0.053$ μm ($n = 15$), with a width/length ratio of 0.63 ± 0.014 μm. Careful examination of the fixed and stained material revealed also the presence of slightly elongated macrospores (Fig. 1A), that averaged 5.72×3.19, ranged from 5.64 to 6.5 μm in length and 2.88 to 4.0 μm in width, and had a mean width/length ratio of 0.55 ± 0.015 ($n = 10$). Macrospores were rare; their occurrence did not exceed 1% of the total number of spores. All these spore measurements are in good accord with a previous study of this microsporidium (Milner, 1972b). Slightly larger average values for measurements of living spores were obtained by Milner, which can be explained by the fact that he did not differentiate macrospores, including them in his morphometric analyses. While being of comparable length with *Paranosema grylli* (c. 4.50 μm) and *Paranosema locustae* (c. 4.95 μm), *P. whitei* spores appeared to be wider (width/length ratio 0.62 versus 0.49 in *P. grylli* and 0.54 in *P. locustae*) and thus can be easily distinguished on smears (Fig. 1A). Interestingly, *Antonospora scoticae* (Fries et al., 1999) which is clustered as a sister group within the same clade with *P. grylli*, *P. locustae*, and *N. whitei* according to SSrDNA-based phylogenies has larger (averaging 6.8×2.7 μm) and more elongated (width/length equaling 0.40) spores, than any of these three species. These data suggest that spore size, especially the width/length index, can be a reliable visual character helpful in differentiating between related species.

3.2. Ultrastructure

Meront (Fig. 1B) ultrastructure is similar to merogonial stages of *P. grylli* and *P. locustae* (Sokolova and Lange, 2002; Sokolova et al., 2003). Round or oval cells measuring 3.8–5.0 μm in diameter were surrounded by a single plasma membrane. Nuclei were in diplokariotic arrangement. Free ribosomes were abundant. Membrane structures were associated with the expansions of perinuclear space. Conglomerates of vesicle-like profiles with coated membranes 30–60 nm in diameter were associated with smooth cisternae, similar to those described previously as meront Golgi organelles for *P. grylli* (Sokolova et al., 2001; Sokolova et al., 2003).

Meront–sporont transitional stages (Figs. 1C–E, 2A) were distinct. Cells were characterized by the appearance of electro-dense inclusions in the nucleoplasm associated with synaptonemal complexes, the markers of the meiotic prophase (Figs. 1C and 2A, inset). Cells with one, two (Figs. 1D and E) or four individual nuclei (not shown) in the view were typical for this phase of the parasite's life cycle, though resolving the nuclear condition (diplokaryotic versus haplokaryotic) is not always feasible on TEM sections. Previous light microscopy studies indicated the presence of haplokaryotic stages in all species of the genus *Paranosema* (Canning, 1953; Milner, 1972a; Sokolova et al., 2003). Haplokaryons might have been produced as a result of two sequential meiotic divisions, which may or may not have been followed by

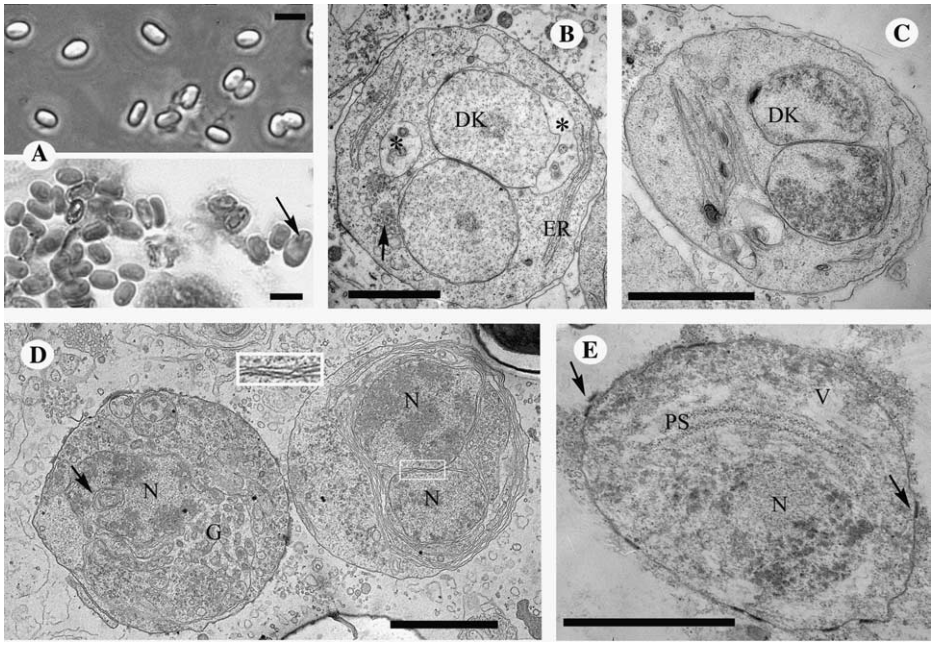

Fig. 1. Light microscopy of spores and fine morphology of presporogonial stages of *P. whitei*. (A) Light microscopy: upper image—fresh spores under phase contrast optics; lower image—methanol fixed spores stained with Trichrome, arrow indicates a macrospore. (B) Diplokaryotic meront; arrow points to Golgi associated with nuclear envelope; note the prominent expansions of the perinuclear space (asterisks). (C) Early diplokaryotic meront–sporont transitional stage; nuclei contain electron dense particles, which are likely associated with synaptonemal complexes. (D) Two transitional stages with nuclei presumably undergoing first meiotic division: in the left cell one invaginated (arrow) nucleus is in the process of karyokinesis, in the neighboring one nuclei have already divided, they lay in close vicinity to each other, though the external membranes of their envelopes do not merge (inset). (E) Transitional stage with one nucleus in the view, displaying some features of sporonts: vacuolization of cytoplasm, appearance of strands of polyribosomes, and deposits of electron-dense material at the outer surface of the plasma membrane (arrows). DK, diplokaryon; ER, endoplasmic reticulum; G, Golgi organelle; N, nucleus; PS, polyribosome strands; V, vacuoles. Bars: A, 5 μm; (B–E), 1 μm; inset D, 4×.

cytokinesis. Synaptonemal complexes were recently discovered and described in *P. grylli* (Nassonova and Smirnov, 2005).

Sporonts and sporoblasts (Figs. 2A–H). Transition to sporogony was marked by deposition of electron-dense amorphous material on the outer surface of the plasma membrane (Figs. 1E and 2A), eventually these patches forming a continuous electron-dense envelope around the parasite. At this stage, parasite cells were diplokaryotic. Another distinguishing feature of the sporonts was vacuolization of the cytoplasm, appearance of strands of polyribosomes and of a cluster of membrane profiles with osmiophilic contents (sporont Golgi organelle, Fig. 2B), which eventually gave rise to vesicles containing polar filament material (Figs. 2F and G). Sporonts divided by binary fission to produce sporoblasts (Fig. 2H). As in *P. grylli* and *P. locustae* at the sporont and sporoblast stages, numerous tubular structures were visible within the host cell cytoplasm surrounding the parasite cell (Figs. 2B–F). They apparently had been derived from the parasite envelope (Figs. 2B–D). Sporonts regularly exhibited pseudopodia-like protrusions (Figs. 2B and C). These protrusions were associated with bands of microtubules located inside the cytoplasm (Figs. 2B and C). The external layer of the sporoblast envelope (a precursor of the exospore) was ornamented with an electron dense matrix (Fig. 2H, inset). This ornamentation was rarely preserved in mature spores.

Spores (Figs. 2I–K) as viewed on ultrathin sections measured c. 3 × 1.5 μm were diplokariotic, possessed and undulating multilayer exospore c.40 nm thick, and an electron lucid endospore 0.35–0.60 μm thick, narrowing apically. Isofilar coils of the polar filament were arranged in one or two rows. Their number, 10–12, was fewer than that of either *P. grylli* (15–22) or *P. locustae* (17–18). The polaroplast was bipartite. As in *P. grylli* and *P. locustae,* a single posterior vacuole was not observed, instead large electron-dense inclusions were located occasionally in the posterior part of the spore (Fig. 2K). The ultrastructural characteristics of spores matched those few reported by Milner (1972a) for the English isolate of *N. whitei*.

Tissue specificity. The fat body of larvae and imagoes was the only site of infection. No signs of gross pathology were observed.

Systematics. *Paranosema whitei*, new combination (Weiser), can be differentiated from other species of the genus by the coleopteran host species, by wider spores (width/length ratio 0.62), and by fewer polar filament coils (10–12).

Paranosema whitei shares following features with *P. grylli* and *P. locustae*: high SSrDNA sequence similarity and similar GC content (Sokolova et al., 2003);

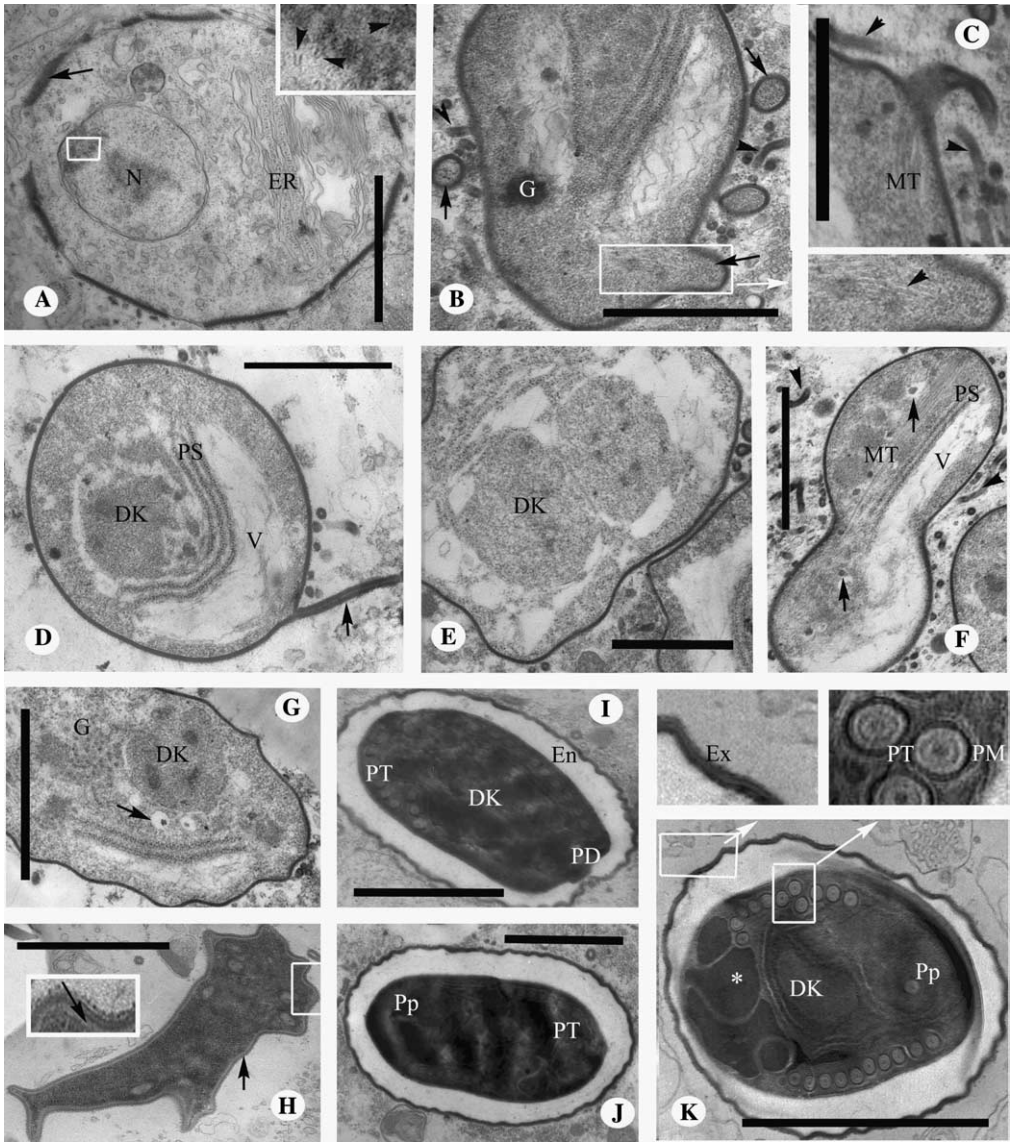

Fig. 2. Morphology of sporogonial stages and spores of *P. whitei*. (A) Transitional stage, electron-dense patches cover the surface of the plasma membrane (black arrow); nucleus contains synaptonemal complexes (inset, arrowheads). (B,C) Sections through sporonts with the continuous electron dense envelopes; pseudopodia-like protrusions (black arrows) contain bands of microtubules (B inset indicated by white arrow, C); tubular structures, abundant in the adjacent host cytoplasm, derive from the sporont envelope (arrowheads). (D) Section through sporont; arrow indicates connection of the tubular structure with the sporont envelope. (E) Sporont undergoing mitosis, condensed chromosomes are visible inside the nucleus. (F) Binary division of the sporont. Arrows indicate membrane containers with the polar tube material, arrowheads—tubular structures in adjacent host cytoplasm. (G), Section through sporont displaying a cluster of membrane profiles (Golgi), which are transformed eventually into to the vacuoles with polar filament material inside (arrow). (H) Sporoblast; electron-lucent endospore appears at this stage between the electron dense envelope and the plasma membrane (arrows); external layer of the wall is ornamented with an electron dense matrix (inset). (I,J) Mature spores with poorly preserved internal structure. (K) Distal end of the spore with electron-dense vacuoles (asterisk). Insets indicated by white arrows, show the structure of polar filament coils and of the multilayered exospore at higher magnification. EN, endospore; EV, electron-dense vacuole; EX, exospore; MT, microtubules; PD, polar disk; PM, plasma membrane; Pp, polaroplast; PT, polar tube; other abbreviations are the same as for Fig. 1. Bars: 1 μm; Insets: A and K, 5×; B and H, 2×.

the diplokaryotic state of nuclei throughout most of development; the presence of a distinct meront–sporont transitional stage with haplokaryotic disposition of the nucleus at least for a short period of time; and production of tubular secretion at the sporont stage. Ultrastructural analysis strongly supports similarity of *N. whitei* to *P. grylli* (Sokolova et al., 2003) and to *P. locustae* (Sokolova and Lange, 2002) predicted on the basis SSU rDNA sequence data. Comparative studies of these three related species provide a good example of agreement of morphological and sequence data, and straightforwardly indicate both placement *N. whitei* inside the genus *Paranosema* and the validity of the proposed combination *P. whitei*. The given ultrastructural description of *N. whitei,* as well

as information presented earlier (Milner, 1972a,b; Weiser, 1953), is in agreement with the genus definition of *Paranosema* except for one point: the number of polar filaments coils in *P. whitei* is 10–12, which is fewer than 15–20 mentioned in the *Paranosema* diagnosis (Sokolova et al., 2003). It may be desirable to remove consideration of the number of polar filament coils from the diagnosis of the genus, while keeping it for resolving species. Because *P. whitei* is a parasite of beetles (Coleoptera) of the genus *Tribolium* (Milner, 1972b) host range of *Paranosema* species is not restricted any more to Orthoptera.

Paranosema or Antonospora? Sequence analysis of SSU rDNA showed, that genus *Antonospora* is closely related to *Paranosema*, which was the reason of nearly simultaneous and confusing reassignment of *N. locustae* to *Paranosema* (Sokolova et al., 2003) and to *Antonospora* (Slamovits et al., 2004). However, *Antonospora* can be differentiated from *Paranosema* species, first, by aforementioned dissimilar size and shape of spores, and, second, there is 3–5% sequence divergence between *P. grylli* and *P. locustae* or *P. whitei*, while the difference between each of these species and *A. scoticae* is about 10% (Sokolova et al., 2003). After all, it is a matter of preference to unite *Paranosema* species and *A. scoticae* in one taxon of the generic level, or to consider them as two separate genera. In the first case, *A. scoticae* will be automatically designated as a type species, but it is poorly described ultrastructurally (Fries et al., 1999), which will create problems in including new species into the genus. Reexamination of *A. scoticae* does not seem feasible, because it was an accidental finding of microsporidian infection in a natural population of wild bees *Andrena scotica* in Sweden (Fries et al., 1999). We treat *Antonospora* and *Paranosema* as two separate but closely related genera, belonging to one supertaxon of the family level.

3.3. Synopsis of the genus Paranosema

Paranosema grylli (Sokolova, Seleznev, Dolgikh, Issi), comb nov. Sokolova et al., 2003, =*Nosema grylli* (Sokolova et al. (1994, p. 493)), type species.
Paranosema locustae (Canning), comb nov. Sokolova et al., 2003, =*Nosema locustae* (Canning (1953, p. 290)), syn. *Antonospora locustae* (Slamovits et al., 2004).
Paranosema whitei (Weiser), new combination for *N. whitei* Weiser (1953, p. 205).

Acknowledgments

Authors are deeply thankful to Margaret C. Henk (Louisiana State University at Baton Rouge) for checking the manuscript for adequate use of English language. Supported by Russian Foundation for Basic research: Grants 04-04-49314 and 03-04-49629.

References

Canning, E.U., 1953. A new microsporidian, *Nosema locustae*, n. sp. from the fat body of the African migratory locust *Locusta migratoria migratorioides*. Parasitology 43, 287–290.

Fries, I., Paxton, R.J., Tengo, J., Slemenda, S.B., da Silva, A.J., Pieniazek, N.J., 1999. Morphological and molecular characterization of *Antonospora scoticae* n. gen., n. sp (Protozoa, Microsporidia) a parasite of the communal bee, *Andrena scotica* Perkins, 1916 (Hymenoptera, Andrenidae). European Journal of Protistology 35, 183–193.

Milner, R.J., 1972a. *Nosema whitei*, a microsporidan pathogen of some species of *Tribolium*.1. Morphology, life-cycle, and generation time. Journal of Invertebrate Pathology 19, 231–238.

Milner, R.J., 1972b. *Nosema whitei,* a microsporidan pathogen of some species of *Tribolium*. 2. Ultrastructure. Journal of Invertebrate Pathology 19, 239–247.

Nassonova, E.S., Smirnov, A.V., 2005. Synaptonemal complexes as evidence for meiosis in the life cycle of the monomorphic diplokaryotic microsporidium *Paranosema grylli*. European Journal of Protistology 41, in press.

Slamovits, C.H., Williams, B.A.P., Keeling, P.J., 2004. Transfer of *Nosema locustae* (Microsporidia) to *Antonospora locustae* n comb based on molecular and ultrastructural data. Journal of Eukaryotic Microbiology 51, 207–213.

Sokolova, J.J., Selesnev, K.V., Dolgikh, V.V., 1994. Microsporidia *Nosema grylli* n.s. from crickets *Gryllus bimaculatus*. Parasitologiya 28, 488–493.

Sokolova, Y., Snigirevskaya, E., Morzhina, E., Skarlato, S., Mironov, A., Komissarchik, Y., 2001. Visualization of early Golgi compartments at proliferate and sporogenic stages of a microsporidian *Nosema grylli*. Journal of Eukaryotic Microbiology, 86S–87S.

Sokolova, Y.Y., Lange, C.E., 2002. An ultrastructural study of *Nosema locustae* Canning (Microspora) from three species of Acrididae (Orthoptera). Acta Protozoologica 41, 229–237.

Sokolova, Y.Y., Dolgikh, V.V., Morzhina, E.V., Nassonova, E.S., Issi, I.V., Terry, R.S., Ironside, J.E., Smith, J.E., Vossbrinck, C.R., 2003. Establishment of the new genus *Paranosema* based on the ultrastructure and molecular phylogeny of the type species *Paranosema grylli* Gen. Nov., Comb. Nov (Sokolova, Selezniov, Dolgikh, Issi 1994), from the cricket *Gryllus bimaculatus* Deg. Journal of Invertebrate Pathology 84, 159–172.

Weiser, J., 1953. Schizogregarinen aus Mehlschadlingen. Acta Societatis Zoologica Bohemoslovenicae 17, 199–211.